BULETINUL INSTITUTULUI POLITEHNIC DIN IAŞI
Publicat de
Universitatea Tehnică „Gheorghe Asachi” din Iaşi
Volumul 63 (67), Numărul 1, 2017
Secția
ELECTROTEHNICĂ. ENERGETICĂ. ELECTRONICĂ

SINGLE-PHASE BUCK DIRECT AC-AC CONVERTER WITH TWO INDUCTANCES AND IMPROVED EFFICIENCY

BY

MIHAI LUCANU, OVIDIU URSARU, CRISTIAN AGHION[*] and NICOLAE LUCANU

Technical University “Gheorghe Asachi” of Iaşi,
Faculty of Electronics, Telecommunications and Information Technology

Received: November 28, 2016
Accepted for publication: December 16, 2016

Abstract. Buck AC-AC converters have numerous applications and are used to control AC motor speed, lighting and heating systems, adjustable AC supplies in commutation, etc. Their characteristics are clearly superior to those of AC variators with thyristors or triacs. They are smaller and lighter, their efficiency is increased and the waveforms of the grid current and of the load voltage are nearly sinusoidal.

Key words: AC chopper; circuit simulation; power electronics; PWM control; switching circuit.

1. Introduction

Several papers present the control and power circuits of AC-AC converters. Reference (Kim *et al*., 1998) presents an improved-commutation buck-boost AC converter and reference (Lucanu *et al*., 2003) analyses a buck converter with IGBTs. Reference (Ursaru *et al*., 2004a) presents a control strategy for harmonic reduction, and (Ursaru *et al*., 2004b) uses simulation to study a three-phase AC-AC converter with IGBTs and fewer power devices. Reference (Yang *et al*., 2008) introduces a three-level converter.

A resonant AC-AC converter using sliding control is suggested by

[*]Corresponding author: *e-mail*: aghion@etti.tuiasi.ro

Garcia *et al*., (2009), while Congwei *et al*., (2009) presents a three-phase converter with 9 IGBTs. The three-phase structure is also approached by Lai *et al*., (2009), which suggests a method for assessing AC-AC converter topologies (Neacşu, 2010). Reference Georgakas and Lafakas, (2010) presents a modified sinusoidal PWM technique aimed at improving the power factor of single-phase AC-AC converters.

References Aurasopon and Piladaeng (2010) and Aurasopon and Khamsen (2013) introduce equivalent circuits for single-phase converters, which allow the calculation of the output capacity in order to obtain a unit power factor at the input (Raţă *et al*., 2009). A new family of three-level choppers is suggested by Li *et al*., (2001), while Thiago *et al*., (2011) presents an input voltage restorer featuring an AC chopper equipped with commercial power modules.

The circuit of an improved-efficiency buck AC-AC converter is analysed by Aghion *et al*., (2012), and Lucanu *et al*., (2014) presenting a boost converter which has an adequate functioning when output impedance varies. Both AC-AC converters have simple control circuits (Valachi *et al*., 2009). Reference Lucanu *et al*., (2014) presents a buck converter with improved switching and its functioning is checked by simulation.

This paper introduces a single-phase buck AC-AC converter with two inductances, which allows to control, at grid frequency, two switching devices, while the other two devices are controlled at high frequency. Both inductances can be wound on the same magnetic core/coil in order to reduce costs. Switching losses are reduced and working frequency can therefore be increased. The correct functioning of the circuit is checked by simulation. We also include useful data and equations for converter design.

2. Circuit Analysis

Fig. 1 presents the power circuit suggested for the single-phase buck AC-AC converter.

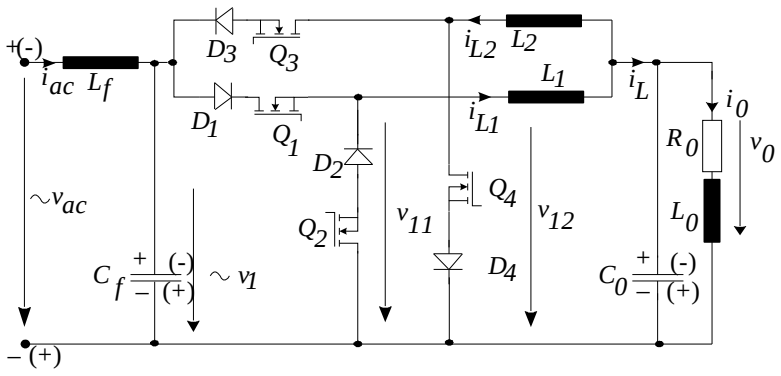

Fig. 1 – The circuit of the single-phase buck AC-AC converter.

In the circuit, L_1 and L_2 are the two buck inductances, MOSs Q_1 and Q_3 are controlled at the converter switching frequency f_S, and MOSs Q_2 and Q_4 are controlled at the AC grid frequency (50 Hz). The components L_f and C_f represent the grid filter, C_0 is the output capacitor and R_0 and L_0 denote the load impedance.

Fig. 2 presents the waveforms of the voltage v_1 at the converter input, of the voltages of the buck inductance, connected in series with the load impedance, during the positive alternation of the grid v_{11} and during the negative alternation v_{12}. It also shows the currents through the buck inductances i_{L1} and i_{L2}, as well as the control signals of the four MOSs.

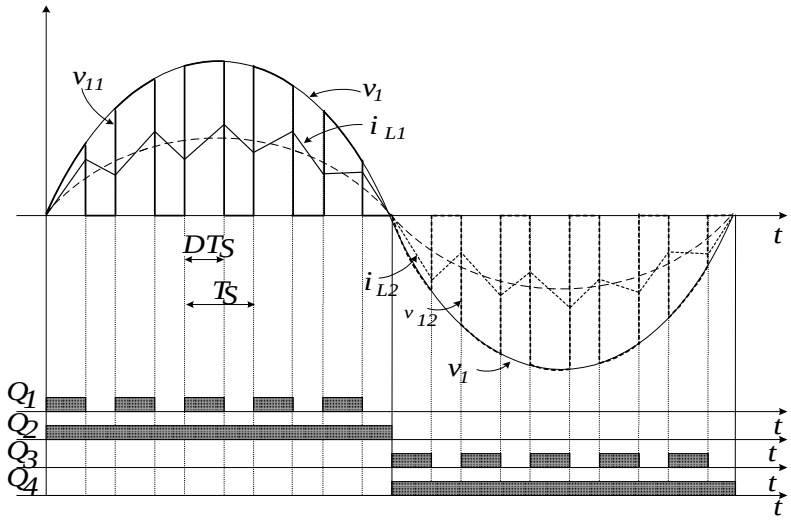

Fig. 2 – Waveforms of the converter input voltages v_1, registered on the buck inductances connected in series with the load inductance v_{11} and v_{12}, of the currents passing through the buck inductances i_{L1}, i_{L2} and of the controls signals of MOSs Q_1–Q_4.

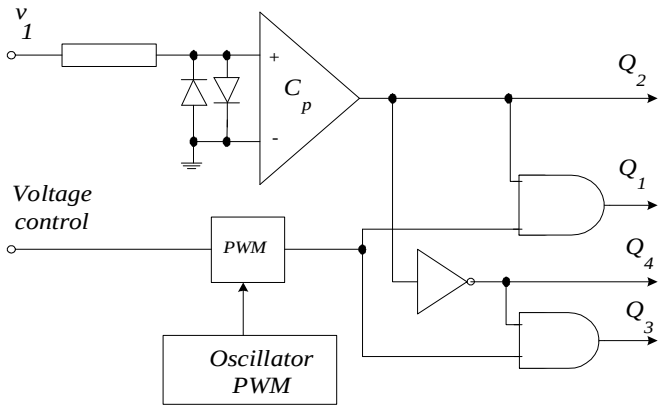

Fig. 3 –The control circuit diagram.

During the positive alternation of the voltage v_1, Q_2 is set in continuous conduction, while Q_1 is under PWM control and the converter operating frequency is set by the sawtooth oscillator (Fig. 3), $f_S = 1/T_S$. MOSs Q_3 and Q_4 are blocked in this interval. During the negative alternation of the voltage V_1, Q_4 is set in continuous conduction, Q_3 is under PWM control, and Q_1 and Q_2 remain blocked. In fact, this control method results in two buck DC-DC converters with antiparallel functioning, which receive power through two diodes only in one alternation of the voltage v_1. By this method, the performance level of AC-AC converters becomes almost as high as the one of DC-DC converters.

The schematic of the control circuit is represented in Fig. 3. It is very simple. In order to avoid the distortion of the waveform of the current i_{ac} supplied by the AC grid, its fundamental must be in phase with the voltage of the grid v_{ac}. This is obtained by adequately choosing the output capacitor C_0. If the ratio between the resistance R_0 and the load inductance L_0 does not change, the phase shift/difference is not influenced by the variation of the duty cycle D. If this ratio changes significantly during operation, an i_L current transducer signal should be applied at the reversing input of the comparator C_p (Fig. 3); thus, the conduction switching between Q_2 and Q_4 takes place when this current crosses the 0 value).

In order to deduce the functioning equations, the voltage v_1 is supposed sinusoidal, MOSs Q_1–Q_4 are supposed to be ideal switches, all circuit components are considered ideal, and voltages v_1 and v_0 remain constant during the T_S switching period. The converter input voltage is given by the following equation:

$$v_1 = \sqrt{2}V_1 \sin \omega t\,,\ \omega = 2\pi f \tag{1}$$

where: v_1 is the actual value of the input voltage (almost equal to the value of the grid voltage 220V), and f is the frequency of the AC grid (f = 50Hz).

The frequency modulation ratio is:

$$m_f = \frac{f_S}{f} = \frac{T}{T_S}, \tag{2}$$

where: T_S and f_S stand for the converter switching period and frequency, respectively.

During the switching period k, the input voltage, assumed to be constant, is:

$$v_{1k} = \sqrt{2}V \sin \omega t_k\,,\ t_k = (k-1)T_S + \frac{T_S}{2}, k = \overline{1, m_f}\,, \tag{3}$$

and the output voltage of the buck converter is:

$$v_{0k} = \sqrt{2}V_0 \sin(\omega t_k - \varphi) = \sqrt{2}DV_1 \sin(\omega t_k - \varphi)\,, \tag{4}$$

where: φ is the phase difference between the fundamentals of voltages v_1 and v_0, and $V_0 = DV_1$ is the rms value of the output voltage.

Based on these simplifying assumptions and considering the voltage on inductor L equal to its average value during a switching period, the following equation is true.

$$Dv_1(t) = L\frac{\mathrm{d}i_L(t)}{\mathrm{d}t} + v_0(t). \tag{5}$$

Eq. (5) equivalent circuit is shown in Fig. 4, where $L = L_1 = L_2$ and $i_L = i_{L1}+i_{L2}$ (as denoted in Fig. 4).

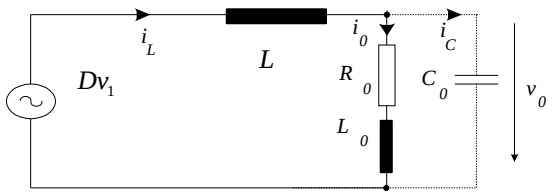

Fig. 4 – Equivalent circuits for buck AC-AC converter.

The following two remarks can be considered for this circuit:

a) the phase difference between the fundamentals of v_1 and i_L is not changed during the variation of duty cycle D and output voltage v_0 correspondingly.

b) the reactance corresponding to inductor L is too small at the frequency of interest, f = 50 Hz, hence v_1 and v_0 have practically similar phases and thus $\varphi = 0$.

To avoid the waveform distortion of the current absorbed from the grid, the current $i_L = i_0 + i_C$ should have the same phase as v_0, in which case C_0 can be computed as follows:

$$C_0 = \frac{L_0}{R_0^2 + \left(\omega L_0\right)^2}. \tag{6}$$

Under these conditions, the converter output circuit will behave as an equivalent resistance given by:

$$R_{0e} = \frac{R_0^2 + (\omega L_0)^2}{R_0}. \tag{7}$$

We suppose that in a practical application, the input voltage varies between the limits:

$$V_{1(\min)} \le V_1 \le V_{1(\max)} \tag{8}$$

and the output voltage should satisfy the limits:

$$V_{0(\min)} \le V_0 \le V_{0(\max)}. \tag{9}$$

With these assumptions, the maximum value for duty cycle D can be computed according to the following expression:

$$D_{(\max)} = \frac{V_{0(\max)}}{V_{1(\min)}} \tag{10}$$

while its minimum value is given by:

$$D_{(\min)} = \frac{V_{0(\min)}}{V_{1(\max)}}. \tag{11}$$

The ripple current flowing through L_1 and L_2 is:

$$\Delta i_L = D(1-D)\frac{v_1}{Lf_s}. \tag{12}$$

The maximum value of this ripple is achieved for D = 1/2 and v_1 = = $\sqrt{2}V_{1\max}$, when $D_{(\min)} \le 1/2 \le D_{(\max)}$, in which case it has the value:

$$(\Delta i_L)_{\max} = \frac{\sqrt{2}V_1(\max)}{4Lf_s}. \tag{13}$$

In case that $D_{(\max)} < 1/2$, the following relation should be used:

$$(\Delta i_L)_{\max} = D_{(\max)}(1-D_{(\max)})\frac{V_{1(\max)}}{Lf_s} \tag{14}$$

and when $1/2 < D_{(\min)}$ the following one:

$$(\Delta i_L)_{\max} = D_{(\min)}(1-D_{(\min)})\frac{V_{1(\max)}}{Lf_s}. \tag{15}$$

The mathematical form of the maximum ripple current presented above can be used to compute the inductances $L_1 = L_2 = L$ by imposing that this ripple current be a percentage of the maximum load current, which is also expressed by:

$$I_{0(\max)} = \frac{V_{0(\max)}}{\sqrt{R_0^2 + (\omega L_0)^2}}. \tag{16}$$

Under the simplifying conditions mentioned hereinabove, the following maximum allowable values are achieved for circuit components, during one switching period k.

The average inductor L_1 current is:

$$I_{L1k\text{AVR}} = \frac{v_{0k}}{R_{0e}} = \frac{DR_0 v_{1k}}{R_0^2 + (\omega L_0)^2}. \tag{17}$$

The average current through transistor Q_1 and the diode D_1 is:

$$I_{Q_1k\text{AVR}} = I_{D_1k\text{AVR}} = DI_{L_1k\text{AVR}} = \frac{D^2 R_0 v_{1k}}{R_0^2 + (\omega L_0)^2}. \tag{18}$$

The average current through transistor Q_2 and the diode D_2 is:

$$I_{Q_2k\text{AVR}} = I_{D_2k\text{AVR}} = (1-D)I_{L_1k\text{AVR}} = \frac{D(1-D)R_0 v_{1k}}{R_0^2 + (\omega L_0)^2}. \tag{19}$$

The maximum repetitive current through the inductor, transistors and diodes is:

$$I_{L_1k\text{RM}} = I_{Q_1k\text{RM}} = I_{D_1k\text{RM}} = I_{Q_2k\text{RM}} = I_{D_2k\text{RM}} = \frac{DR_0 v_{1k}}{R_0^2 + (\omega L_0)^2} + \frac{D(1-D)v_{1k}}{2Lf_s}. \tag{20}$$

The voltage stress of transistor Q_1 and the reverse voltage applied to diode D_2 is:

$$V_{Q_1\text{RM}} = V_{D_2\text{RRM}} = v_{1K}. \tag{21}$$

The transistors Q_3 and Q_4 are switched off during this half cycle. The reverse voltage applied to D_3 and the forward voltage applied to Q_4 are as follows:

$$V_{D_3\text{RRM}} = v_{1K} - v_{0k} = (1-D)v_{1k},\ v_{Q4\text{RM}} = v_{0k} = Dv_{1k}. \tag{22}$$

Taking into account that v_{1k} has harmonic variation and all transistors and diodes are conducting during a half cycle of the grid voltage, the following values are achieved for maximum voltage and current stress of the components.

The maximum repetitive current through inductors, transistors and diodes are computed based on eq. (20), which is strictly dependent on both v_{1k} and D. Its maximum value is achieved for:

$$v_{1K} = \sqrt{2}V_{1(\max)} \quad \text{and} \quad D_1 = \frac{1}{2} + \frac{R_0 Lf_s}{R_0^2 + (\omega L_0)^2} \tag{23}$$

and is computed with one of the following equations:

$$I_{\mathrm{LRM}} = I_{\mathrm{QRM}} = I_{\mathrm{DRM}} = \begin{cases} \dfrac{D_{(\min)} R_0 \sqrt{2} V_{1(\max)}}{R_0^2 + (\omega L_0)^2} + \dfrac{D_{(\min)}(1 - D_{(\min)})}{2Lf_s}, \text{ if } D_1 < D_{(\min)}; \\ \dfrac{D_1 R_0 \sqrt{2} V_{1(\max)}}{R_0^2 + (\omega L_0)^2} + \dfrac{D_1(1 - D_1)}{2Lf_s}, \text{ if } D_{(\min)} < D_1 < D_{(\max)}; \\ \dfrac{D_{(\max)} R_0 \sqrt{2} V_{1(\max)}}{R_0^2 + (\omega L_0)^2} + \dfrac{D_{(\max)}(1 - D_{(\max)})}{2Lf_s}, \text{ if } D_{(\max)} < D_1. \end{cases} \quad (24)$$

The maximum average repetitive current through Q_1, Q_3, D_1 and D_3 is computed based on eq. (18) and becomes as follows:

$$I_{Q_1\,\mathrm{AVR}} = I_{Q_3\,\mathrm{AVR}} = I_{D_1\mathrm{AVR}} = I_{D_3\,\mathrm{AVR}} = \frac{D_{(\max)}^2 R_0 \sqrt{2} V_{1(\max)}}{\pi \left[R_0^2 + (\omega L_0)^2 \right]}. \quad (25)$$

The maximum average current through Q_2, Q_4, D_2 and D_4 is computed based on eq. (19), which depends on v_{1k} and D:

$$I_{Q_2\mathrm{AVR}} = I_{Q_4\mathrm{AVR}} = I_{D_2\mathrm{AVR}} = I_{D_4\mathrm{AVR}} = \begin{cases} \dfrac{D_{(\min)}(1 - D_{(\min)})\sqrt{2} V_{1(\max)}}{2\pi L f_s}, \text{ if } D_{(\min)} > \dfrac{1}{2}; \\ \dfrac{\sqrt{2} V_{1(\max)}}{8\pi L f_s}, \text{ if } D_{(\min)} < \dfrac{1}{2} < D_{(\max)}; \\ \dfrac{D_{(\max)}(1 - D_{(\max)})\sqrt{2} V_{1(\max)}}{2\pi L f_s}, \text{ if } D_{(\max)} < \dfrac{1}{2}. \end{cases} \quad (26)$$

The maximum average current through L_1 and L_2 is computed based on eq. (17) and is given by:

$$I_{L_1\,\mathrm{AVR}} = I_{L_2\,\mathrm{AVR}} = \frac{D_{(\max)} R_0 \sqrt{2} V_{1(\max)}}{\pi \left[R_0^2 + (\omega L_0)^2 \right]}. \quad (27)$$

The maximum repetitive voltages applied to Q_1 and Q_3 are, according to eq. (21), as follows:

$$V_{Q_1\,\mathrm{RM}} = V_{Q_3\,\mathrm{RM}} = \sqrt{2} V_{1(\max)}. \quad (28)$$

The maximum reverse voltages applied to D_1 and D_3 are, according to eq. (22), as follows:

$$V_{D_1 R\,\mathrm{RM}} = V_{D_3 R\,\mathrm{RM}} = (1 - D_{(\min)})\sqrt{2} V_{1(\max)}. \quad (29)$$

The maximum repetitive voltages applied to Q_2 and Q_4 are, according to eq. (22), as follows:

$$V_{Q_2\text{RM}} = V_{Q_4\text{RM}} = D_{(\max)}\sqrt{2}V_{1(\max)}. \tag{30}$$

The maximum reverse voltages applied to D_2 and D_4 are, according to eq. (21), as follows:

$$V_{D_2R\text{RM}} = V_{D_4R\text{RM}} = \sqrt{2}V_{1(\max)}. \tag{31}$$

3. Simulation Results

The right functioning of the circuit was tested by simulation with a resistive load R_0 = 100 ohm and a inductive load L_0 = 100 mH.

The components of the simulated circuit have the following values: input inductive L_f = 7 mH, input capacitor C_f = 3.5 uF, output capacitor C_0 = = 10 uF , the buck inductances L_1 = L_2 = 1.5 mH. The amplitude of the grid voltage is 110 V and the switching frequency is f = 40 KHz.

The simulations took into account the following values of the duty cycle: D = 0.3, 0.5, and 0.7. The paper presents only some of the waveforms obtained, namely the most representative ones. Thus, Fig. 5 shows the waveforms of the v_{ac} grid voltage and of the v_0 load voltage, as well as the waveforms of the i_{ac} current supplied by the grid and the i_0 load current for D = 0.3.

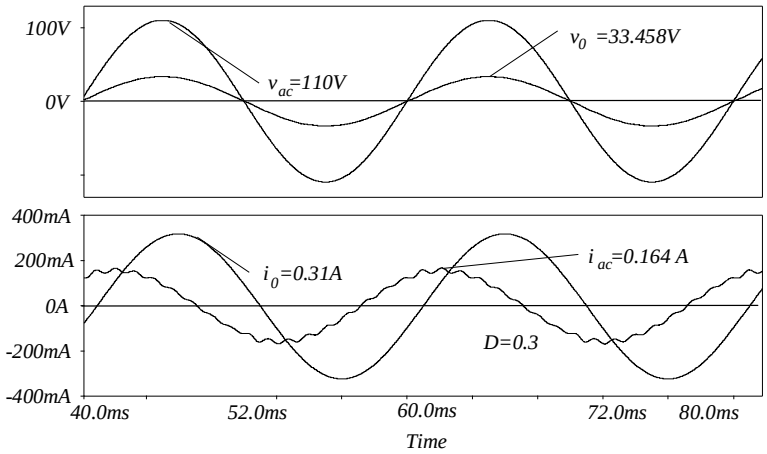

Fig. 5 – Waveforms of the v_{ac} voltage, v_0 voltage, i_{ac} current and i_0 current, for D = 0.3.

Fig. 6 presents the same waveforms for D = 0.5.

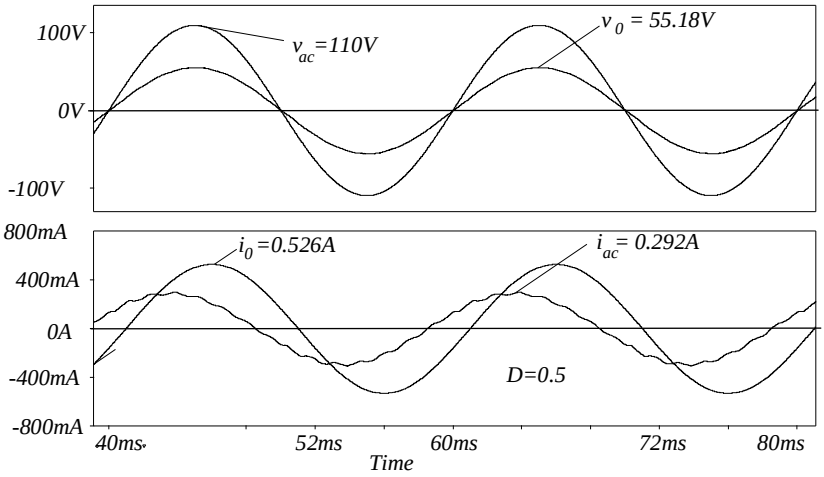

Fig. 6 – Waveforms of the v_{ac} voltage, v_0 voltage, i_{ac} current and i_0 current, for D = 0.5.

Fig. 7 presents the same waveforms for D = 0.7. The waveforms of the load voltage and current are nearly sinusoidal.

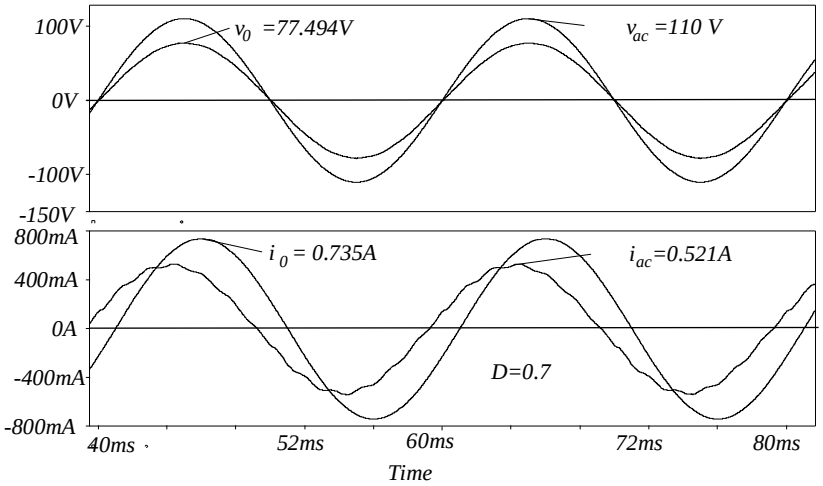

Fig. 7 – Waveforms of the v_{ac} voltage, v_0 voltage, i_{ac} current and i_0 current, for D = 0.7.

Fig. 8 shows the efficiency variation depending on the D duty cycle, based on the simulation results. We notice thus that the efficiency is high for all the values of D.

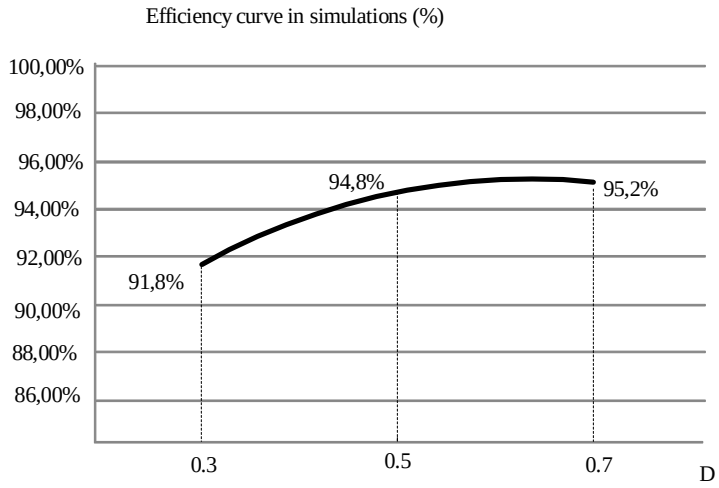

Fig. 8 – Variation of the efficiency depending on the *D* duty cycle.

Fig. 9 shows the variations V_0/V_1 depending on the *D* duty cycle, tested by simulation vs. theoretical.

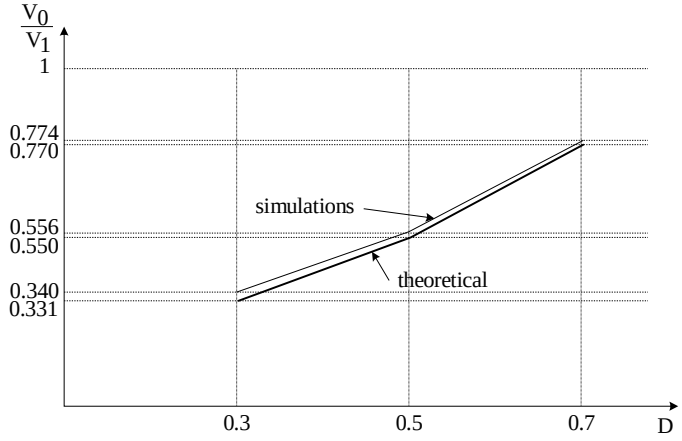

Fig. 9 – Variations V_0/V_1 depending on the *D* duty cycle.

4. Conclusions

This paper presents the analysis and simulation of a buck AC-AC converter with four controlled transistors, two of them in conduction in one half-period of the sinusoidal alternation. The adequate functioning of the circuit was tested by simulation for various values of the control factor of the MOS

transistors. Based on the various values of the control factor D = 0.3, 0.5 and 0.7, we presented the main waveforms of the voltages and of the input and output currents, as well as the variation of the converter energy efficiency.

REFERENCES

Aghion C., Lucanu M., Ursaru O., Lucanu N., *Direct AC-AC Step-Down Single-Phase Converter with Improved Performances*, Electronics and Electrical Engineering, **18**, *10*, 33-36 (2012).

Aurasopon A., Khamsen W., *Improvement of Input Power Factor in PWM AC Choppers by Selecting the Optimal Parameters*, Przeghed Elektrotechiczny, ISSN 0033-2097, R89, **10**, 2013, 210-216.

Aurasopon A., Piladaeng N., *Unity Input Power Factor for a PWM Boost AC Chopper*, I.E.E.T.A, **1**, *3*, 135-140 (2010).

Congwei L., Bin W., Zargari N. R., Devei X., and Jiacheng W., *A Novel Three-Phase Three Leg AC/AC Converter Using Nine IGBT's*, IEEE Trans. on Power Electron., **24**, *5*, 2009, 1151-1160.

Garcia de Vicuna L., Castilla M., Miret J., Matas J., Guerrero J. M., *Sliding Mode Control for a Single-Phase AC/AC Quantum Resonant Converter*, IEEE Trans. on Ind. Electron., **56**, *6*, Sept. 2009, 3496-3504.

Georgakas K., Lafakas A., *Modified Sinusoidal Pulse width Modulation Operation Technique of an AC-AC Single-Phase Converter to Optimize the Power Factor*, I.E.T. Power Electronics, **3**, *3*, 2010, 454-464.

Kim J.H., Min B.D., Kwon B.H., Won S.C., *A PWM Buck-Boost AC Chopper Solving the Commutation Problem*, I.E.E.E. Trans. on Ind. Electron., **45**, 5, 1998, 832-835.

Lai R., Wang F., Burgos R., Pei Y., Boroyevich D., Wang B., Lipo T.A., Immanuel V.D., Karimi K.J., *A Systematic Topology Evaluation Methodology for High-Density Three-Phase PWM AC-AC Converters*, IEEE Trans. on Power Electron., **24**, *7*, 2009, 1671-1681.

Li L., Yang Y., Zhong Q., *Novel Family of Single-Stage Three Level A.C. Choppers*, I.E.E.E. Trans. on Power Electron., **26**, *2*, 2001, 504-511.

Lucanu M., Ursaru O., Aghion C., Lucanu N., *Single Phase Direct AC-AC Boost Converter*, Adv. in Electrical a. Computer Engng. J., Suceava, **14**, *3*, 107-112 (2014).

Lucanu M., Ursaru O., Aghion C., Lucanu N., *Single Phase Direct AC-AC Step-Down Converter*, IET Power Electronics, **7**, *12*, 2014, 3101-3109.

Lucanu M., Ursaru O., Aghion C., *Single Phase A.C. Choppers with I.G.B.T's*, Proc. of the Internat. Symp. on Signal, Circ. a. Syst. SCS 2003, July 10-11, 2003, 213-216.

Neacşu D. O., *Analytical Investigation of a Novel Solution to AC Waveform Tracking Control*, IEEE Internat. Symp. on Industrial Electronics, 2010, 2684-2689.

Rață G., Rață M., Graur I., Milici D.L., *Induction Motor Speed Estimator Using Rotor Slot Harmonics*, Adv. in Electrical a. Computer Engng. J., Suceava, **9**, 1, 70-73 (2009).

Thiago B. Soliero, Clovis A. Petry, Joao C. dos S. Fagundes, Yvo Barbi, *Direct AC-AC Converters Using Commercial Power Modules Applied to Voltage Restorers*, IEEE Trans. on Ind. Electron., **58**, *1*, 2011, 278-288.

Ursaru O., Lucanu M., Aghion C., Tigăeru L., *Three-Phase AC Chopper with I.G.B.T's,with the Load Connected in Star Shape with Ground Wire*, Bul. Inst. Politehnic, Iaşi, **L(LIV)**, *1-2*, 87-97 (2004).

Ursaru O., Lucanu M., Tigăeru L., Aghion C., *PWM Sinusoidal Harmonic Injection Control Strategy for a Single Phase AC Chopper*, Bul. Inst. Politehnic, Iaşi, **L(LIV)**, *1-2*, 79-86 (2004).

Valachi A., Timiş M., Danubianu M., *Some Contributions to Synthesis and Implementation of Multifunctional Registers*, 11th WSEAS Internat. Conf. on Automatic Control, Modelling & Simulation (acmos'09), Istanbul, Turkey, 2009, 146-149.

Yang J. D., Li L., Yang K. M., *Anovel Buck-Boost Mode Single Stage Three Lavel AC/AC Converter*, IEEE Indus. Electro. (IECON), 596-600, 2008.

CONVERTOR DIRECT AC-AC BUCK MONOFAZAT CU DOUĂ INDUCTANȚE ȘI RANDAMANET ÎMBUNĂTĂȚIT

(Rezumat)

Convertoarele AC-AC buck au cele mai multe aplicații și se folosesc în comanda turației motoarelor de curent alternativ, controlul încălzirii electrice și a iluminatului, surse reglabile de curent alternativ în comutație, etc. Convertorul propus realizat cu tranzistoare MOS oferă performanțe mult mai bune decât variatoarele de curent alternativ realizate cu tiristoare sau triacuri. Utilizarea strategiilor de comandă de tip PWM din care două câte două tranzistoare sunt comandate doar pe o semi-alternanță, ne permite obținerea unui randament mai bun în comparație cu strategiile clasice de comandă a variatoarelor de tensiune alternativă. Formele de undă ale curentului absorbit de la rețea și a tensiunii de sarcină sunt practic sinusoidale, iar caracteristica de reglaj a convertorului, obținută prin simulare, urmărește îndeaproape caracteristica de reglaj teoretică.